

# Dynamic 2D implementation of 3D diffractive optics: supplementary material

HAIYAN WANG AND RAFAEL PIESTUN\*

Department of Electrical, Computer, and Energy Engineering, University of Colorado Boulder, Boulder, Colorado 80309, USA

\*Corresponding author: [piestun@colorado.edu](mailto:piestun@colorado.edu)

Published 2 October 2018

This document provides supplementary information to “Dynamic 2D implementation of 3D diffractive optics,” <https://doi.org/10.1364/OPTICA.5.001220>. It presents additional information on diffraction efficiency analysis, system limits discussion, and experiment details of 3D diffractive optics.

## 1. DIFFRACTION EFFICIENCY ANALYSIS

3D diffractive optics has several interesting advantages relative to thin DOEs in terms of diffraction efficiency, spectral/angular selectivity, as well as new functionalities such as synthetic 3D spatial-temporal wavefront encoding, engineered space-variant functions, and space-time pulse shaping. Here we show the diffraction efficiency can be controlled and enhanced by proper design, due to the additional degrees of freedom provided by the third dimension, compared to 2D DOEs.

The system parameters of importance are the number of layers,  $N$ , layer separation,  $\Delta z$ , pixel sizes in the  $x$  and  $y$  directions,  $\Delta x$  and  $\Delta y$ , and number of pixels in the  $x$  and  $y$  directions,  $N_x$  and  $N_y$ . For the examples shown here,  $\Delta x = \Delta y = 8\mu\text{m}$ ,  $\Delta z = 486\mu\text{m}$ . We change  $N=2, 4, 6, \dots, 20$ ,  $N_x = N_y = 256, 1024$ .

We implement a frequency multiplexing scheme with two wavelengths,  $633\text{nm}$  and  $532\text{nm}$ , to encode two desired reconstruction functions. For the purpose of investigating diffraction efficiency, the target images are two off-axis spots at different locations. The first (second) spot, which corresponds to the  $633\text{nm}$  ( $532\text{nm}$ ) illuminating wavelength is located halfway (three quarters) from the center to the edge of the far-field grid used.

The 3D diffractive optics are designed with the POCS algorithm with distribution-on-layers optimization. The two spots are reconstructed as designed, namely the first spot (left) shows up for  $633\text{nm}$  wavelength reconstruction, and the second one (right) for  $532\text{nm}$ . The diffraction efficiency of both spots as functions of the number of layers and the number of pixels are shown in Fig. S1.

It takes less than 1 minute to finish the design at two layers with  $256 \times 256$  pixels, on a 2.8GHz quad-core CPU with 12Gb memory. The diffraction efficiencies for the two spots are 64.55% and 66.68%, respectively. As the number of layers increased to 20, the diffraction efficiencies increased to 70.28% and 72.07%,

respectively. As we use  $1024 \times 1024$  pixels in each layer, the diffraction efficiencies for the two spots are 74.11% and 75.16%, respectively, when the number of layer is 2. The numbers increase to as large as 83.26% and 84.77%, respectively, as 6 layers are used in the design. Designs with more layers are beyond the computational power of a personal computer but are still possible with more powerful hardware.

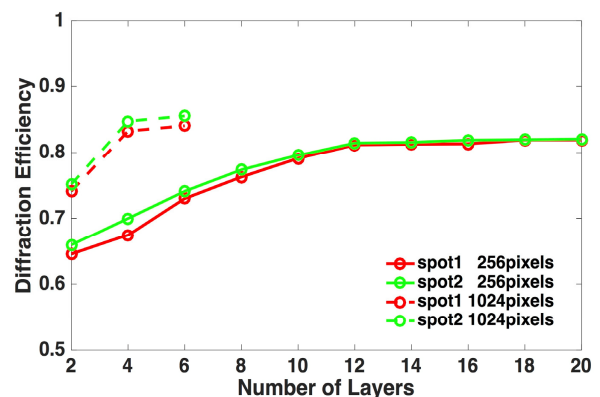


**Fig. S1.** Diffraction efficiency as functions of the number of layers and the number of pixels in each layer. The solid red line is the diffraction efficiency of the first spot as a function of the number of layers with  $256 \times 256$  pixels. The solid green line is the diffraction efficiency of the second spot as a function of the number of layers with  $256 \times 256$  pixels. The dashed red line is the diffraction efficiency of the first spot as a function of the number of layers with  $1024 \times 1024$  pixels. The dashed green line is the diffraction efficiency of the second spot as a function of the number of layers with  $1024 \times 1024$  pixels.

This result, like all other results, confirms the hypothesis that 3D diffractive optics indeed provides additional degrees of freedom to enhance system performance such as diffraction efficiency. One

would expect further improvements in diffraction efficiency with more layers and more pixels.

## 2. SLM DEVIATIONS AND MISALIGNMENT ANALYSIS

SLMs are common devices for light manipulation purposes. In particular, reflective SLMs are more popular because of shorter response time and higher fill factor. The ideal phase-only reflective SLM addresses arbitrary phase profiles onto a coherent light beam. However, the reflective display panels usually suffer deviations between the applied voltages and the designed phase values, due to the non-ideal production process [1–3]. Those distortions could lead to performance degradation. Here, we investigate the effect of SLM phase drifts on 3D diffractive optics in terms of diffraction efficiency and relative error.

The 3D diffractive optics is designed of 2 layers with  $128 \times 128$  pixels in each layer. Letter “C” and “U” in a frequency multiplexing scheme, namely “C” with  $633\text{nm}$  illumination and “U” with  $532\text{nm}$  illumination. The pixel size is  $8\mu\text{m} \times 8\mu\text{m}$ , and the layer separation is  $486\mu\text{m}$ . The simulation yields diffraction efficiencies of 62.5% for “C” and 65.5% for “U”, with a relative error of 0.16 and 0.14 respectively.

The investigation is conducted in three aspects. The results are shown in Fig. S2. First, we test the linear deviation. This applies to an SLM that is not properly calibrated, or the wavelength or direction of the incident beam is drifted from the designed value. The result is the phase modulation from the SLM is linearly shifted from the original by a constant coefficient. We set the coefficient to be 0.8, 0.6, and the 0.4, as is shown in Fig. S2a. The corresponding diffraction efficiencies for the far-field pattern decrease as the deviation becomes larger and as more energy being transferred to the DC term. Accordingly, as expected, the relative error increases. Second, we test the effect of a nonlinear deviation in the SLM phase. This occurs when there are errors in the look-up table which is a built-in mechanism in the SLM’s control circuit to linearly convert the gray level of the input phase pattern to the resulting phase retardation of the liquid crystal molecule by properly adjusting the applied voltage. The phase map of the designed layers are converted in a nonlinear fashion, for the 2<sup>nd</sup>, 3<sup>rd</sup>, and 4<sup>th</sup> order, as is shown in Fig. S2b. The diffraction efficiencies drop more as higher order nonlinear deviations are induced. A stronger DC term shows up as well as larger errors are being generated.

Third, we add random noise with different levels to the phase map. This is to simulate irregularities of liquid crystal cells, which cause a spatially varying phase response of the SLM. Fig. S2c shows results for random noise levels of 20%, 40%, and 60%. The diffraction efficiencies of both patterns are impaired as the noise level increases, and speckles start to appear in the background.

Last, we investigate the effect of misalignment between the two layers. The design is up-sampled 8 times such that modeling of the layer can be shifted distances as small as  $1\mu\text{m}$ . Visualization 2 shows the reconstructed pattern under both  $633\text{nm}$  and  $532\text{nm}$  illumination as the second layer is misaligned from  $-20\mu\text{m}$  to  $20\mu\text{m}$ . The corresponding diffraction efficiency and relative error are plotted in Fig. S3a. The results show that with 2 layers, the misalignment tolerance could be up to 1 pixel ( $8\mu\text{m}$ ) and still yield acceptable reconstructed patterns. Visualization 3 shows the alignment tolerance in longitudinal direction. In frequency multiplexing scheme, the second layer is misaligned from  $-50\mu\text{m}$  to  $50\mu\text{m}$  with respect to the  $486\mu\text{m}$  layer separation in the design. The diffraction efficiency and relative error are plotted in Fig. S3b. Acceptable reconstructed patterns are obtained from in the

misalignment range from  $-25\mu\text{m}$  to  $25\mu\text{m}$ . Alignment tolerances become more critical as the number of layers is increased.

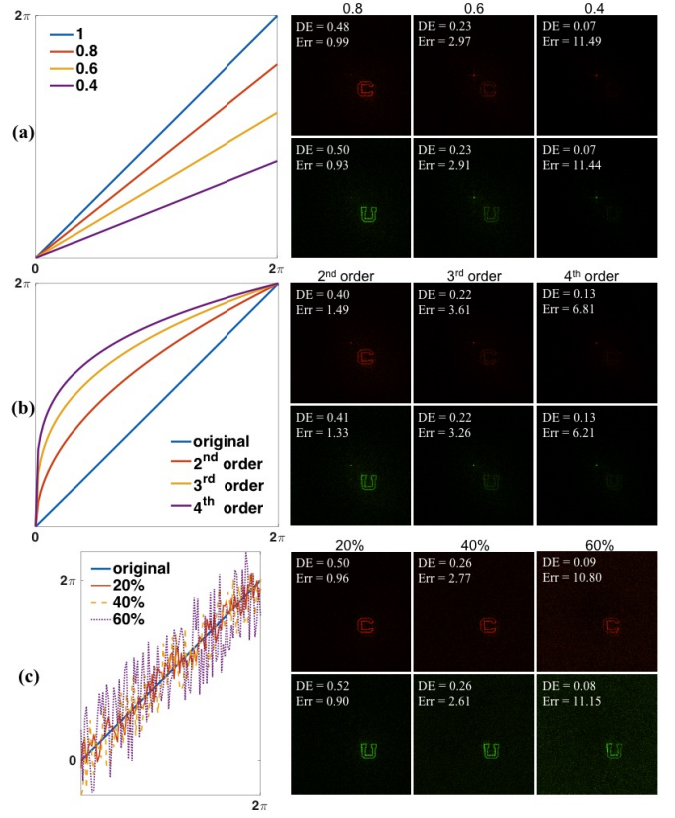


**Fig. S2.** Simulation results for SLM phase deviation analysis. (a) linear deviation of the phase map of 20% (0.8), 40% (0.6), and 60% (0.4) with the corresponding reconstructed images. (b) phase map of nonlinear deviation of 2<sup>nd</sup>, 3<sup>rd</sup>, and 4<sup>th</sup> order with the corresponding reconstructed images. (c) phase map with added random noise at levels of 20%, 40%, and 60% with the corresponding reconstructed images.

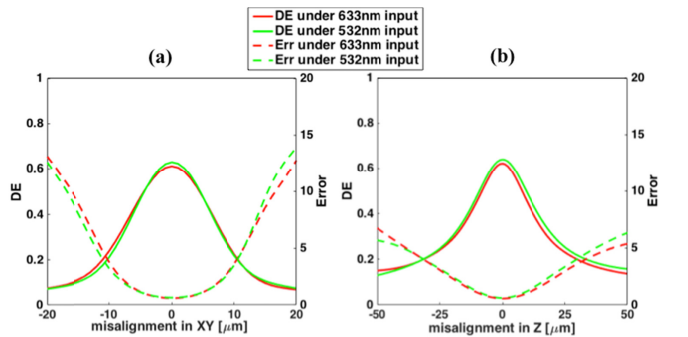


**Fig. S3.** Simulation results for layer misalignment analysis. The diffraction efficiency and relative error of the two far-field patterns, corresponding to  $633\text{nm}$  and  $532\text{nm}$  in a frequency-multiplexing scheme, are plotted as a function of relative shifting distance between the two designed layers.

## 3. MULTIPLEXING LIMITS

Angular and frequency multiplexing are the two important functionalities of the proposed 2D implementation of 3D diffractive optics. Here, we provide a discussion on the impact of the interval between the multiplexed angles or wavelengths on the crosstalk of the encoded information. We design 3D diffractive optics consisting of 4 layers, with  $128 \times 128$  pixels on each layer. We vary the angular interval in angular multiplexing, from  $0.02^\circ$  to

$1^\circ$ , and plot the normalized error as a function of angular interval. Fig. S4 (left) shows the plot and reconstructed images, from which we conclude the smallest angular interval to avoid severe crosstalk in this example is  $\sim 0.2^\circ$ .

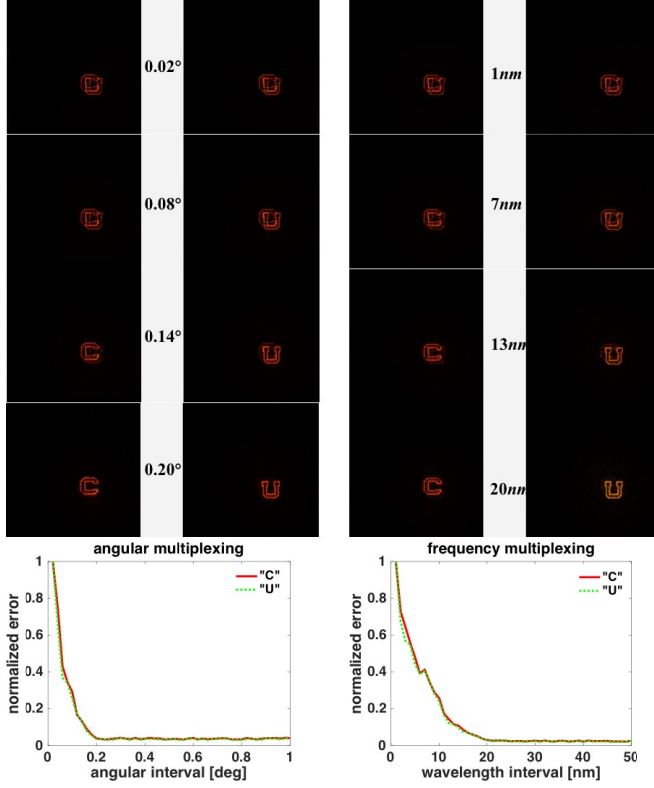


**Fig. S4.** Crosstalk measurement for angular multiplexing (left) and frequency multiplexing (right). Top left: The reconstructed images are displayed for designs at selected angle intervals. Bottom left: Normalized error in angular multiplexing as a function of angular interval between the two reconstructions. Top right: The reconstructed images are displayed for designs at selected wavelength intervals. Bottom right: Normalized error in wavelength multiplexing as a function of wavelength interval between the two reconstructions.

In frequency multiplexing, we use the same parameters for the 3D diffractive optics, and encode “C” at  $633nm$  while changing the encoding wavelength for “U” from  $632nm$  to  $583nm$ . The normalized error and reconstructed images for designs at selected wavelength intervals are shown in Fig. S4 (right). We conclude the smallest wavelength interval to avoid severe crosstalk in this case is  $\sim 20nm$ .

#### 4. EXPERIMENTAL DETAILS

For the design of the 7-function frequency multiplexing diffractive optics presented in the main text, we expanded the number of pixels in each layer to  $256 \times 256$  to prevent crosstalk among the multiplexed output fields. Accordingly, the beam size was adjusted to  $3mm$ . To suppress the background light unaffected by the SLM, the designed layers are padded with tilted blazed gratings. The results are shown in Fig. S5.

The SLM is horizontally divided into two parts, left and right, to accommodate both layers. The beam first incident on the right part where the first layer is displayed, then imaged by a concave spherical mirror at a small distance front of the left part, where the second layer is displayed. Fig. S5 left is the photo of experimental implementation.

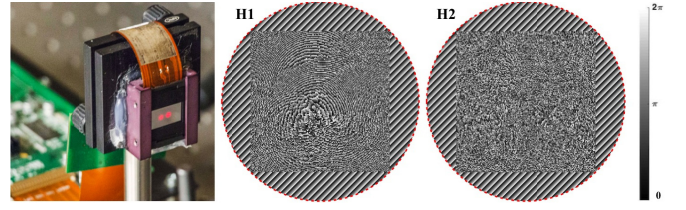


**Fig. S5.** Designed layers for frequency multiplexing with 7 wavelengths. The continuous phase patterns are padded with tilted blazed gratings to match with the beam profile (indicated by red dashed circle) while suppressing the background of light unaffected by the SLM.

#### 5. DESIGN OF 16-LAYER 3D DIFFRACTIVE OPTICS

In this section, we present the results of a design for a 16-layer 3D diffractive optics for frequency multiplexing of 2 functions, namely the letters “C” and “U” from the “CU” logo, with  $633nm$  and  $532nm$  illumination, respectively. Fig. S6 shows the designed phase patterns, which improves the diffraction efficiency of the two far-field images to reach 77.4% and 81.8% from 62.1% and 65.4%.

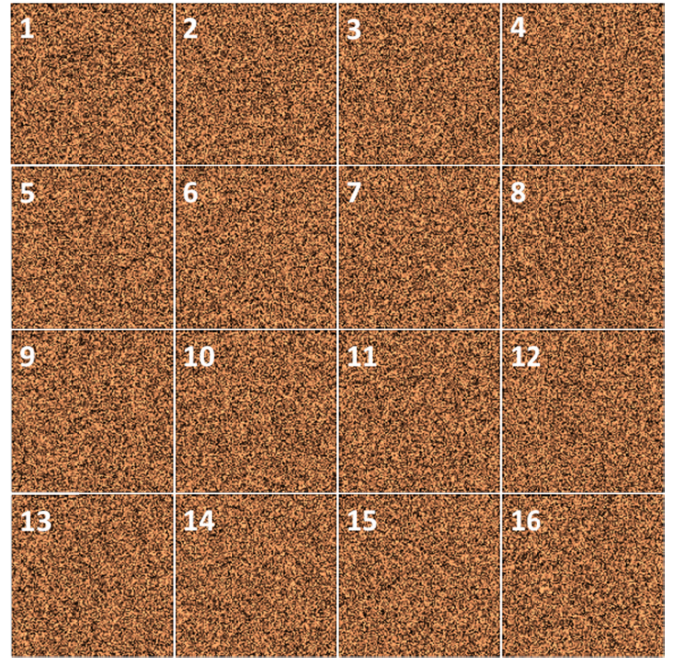


**Fig. S6.** Phase patterns of 3D diffractive optics with 16 layers. The device is designed to multiplex “C” and “U” in frequency. The pixel number in each layer is  $128 \times 128$ , and the phase values are 8 bits.

#### References

1. Z. Zhang, Z. You, and D. Chu, "Fundamentals of phase-only liquid crystal on silicon (LCOS) devices," *Light Sci. Appl.* **3**, e213 (2014).
2. D. Engström, M. Persson, J. Bengtsson, and M. Goksör, "Calibration of spatial light modulators suffering from spatially varying phase response," *Opt. Express* **21**, 16086–16103 (2013).
3. R. K. Banyal and B. R. Prasad, "Nonlinear response studies and corrections for a liquid crystal spatial light modulator," *Pramana* **74**, 961–971 (2010).